ORGANIC LETTERS

2012
Vol. 14, No. 11
2854–2857

Aetheramides A and B, Potent HIV-Inhibitory Depsipeptides from a Myxobacterium of the New Genus "*Aetherobacter*"

Alberto Plaza,[†] Ronald Garcia,[†] Giuseppe Bifulco,[‡] Javier Pablo Martinez,[§] Stephan Hüttel,[†] Florenz Sasse,[∥] Andreas Meyerhans,[§] Marc Stadler,[⊥] and Rolf Müller*,[†]

Department of Microbial Natural Products, Helmholtz Institute for Pharmaceutical Research Saarland, Institut für Pharmazeutische Biotechnologie, Universität des Saarlandes, Postfach 151150, 66041 Saarbrücken, Germany, Dipartimento di Scienze Farmaceutiche e Biomediche, Universitá di Salerno, via Ponte don Melillo, 84084 Fisciano (SA), Italy, Department of Experimental and Health Sciences, ICREA Infection Biology Laboratory, Universitat Pompeu Fabra, Doctor Aiguader, 88, Edificio PRBB, 08003 Barcelona, Spain, and Departments of Chemical Biology and Microbial Drugs, Helmholtz Centre for Infection Research, Inhoffenstrasse 7, 38124 Braunschweig, Germany

rom@mx.uni-saarland.de

Received April 25, 2012

ABSTRACT

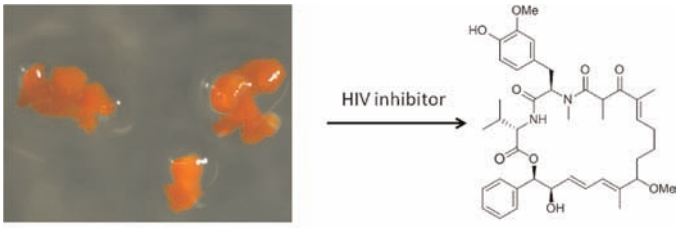

Aetherobacter rufus Aetheramide A

Aetheramides are structurally distinctive cyclic peptides isolated from a novel myxobacterial genus proposed to be termed "*Aetherobacter*". The structures were solved by a combination of NMR analyses, quantum mechanical calculations, and chemical derivatizations. Aetheramides which contain a unique polyketide moiety and two amino acid residues potently inhibited HIV-1 infection with IC_{50} values of ~0.015 μM. Furthermore aetheramides showed cytostatic activity against human colon carcinoma (HCT-116) cells with IC_{50} values of 0.11 μM.

Natural products may be used as leads and scaffolds for elaboration of new utrgently needed drugs to combat infectious diseases which are the main cause of death worldwide.[1] Myxobacteria have proven to be an excellent source of secondary metabolites, many of which originate from mixed polyketide-nonribosomal peptide biosynthetic pathways.[2] These natural products are characterized by showing both unique structures and novel modes of action.[3] Recently, we reported the discovery of a new

[†] Department of Microbial Natural Products, Helmholtz Institute for Pharmaceutical Research Saarland, Institut für Pharmazeutische Biotechnologie.
[‡] Dipartimento di Scienze Farmaceutiche e Biomediche, Universitá di Salerno.
[§] Department of Experimental and Health Sciences, ICREA Infection Biology Laboratory, Universitat Pompeu Fabra.
[∥] Department of Chemical Biology, Helmholtz Centre for Infection Research.
[⊥] Department of Microbial Drugs, Helmholtz Centre for Infection Research.

(1) Rasko, D. A.; Sperandio, V. *Nat. Rev. Drug Discovery* **2010**, *9*, 117.
(2) Wenzel, S. C.; Müller, R. *Curr. Opin. Drug Discovery Dev.* **2009**, *12*, 220.
(3) Weissman, K. J.; Müller, R. *Nat. Prod. Rep.* **2010**, *27*, 1276.

10.1021/ol3011002
Published on Web 05/22/2012

myxobacterial genus for which we proposed the name "*Aetherobacter*".[4] This new genus is closely related to *Sorangium*, which is one of the most prolific producers of active natural products among myxobacteria.[5] *A. rufus* (SBSr003) is the first strain from this new genus to be chemically studied. It was cultivated in a yeast-based medium,[6] and LC-MS analysis of the ethyl acetate extracts showed the presence of two major compounds containing peptidic fragments and possessing the same molecular formula. Moreover, antifungal activity and cytotoxic effects against a human colon tumor cell line (HCT-116) were observed in these extracts. Bioassay (cytotoxicity) and ^{1}H NMR guided fractionation led to the isolation of two new unusual depsipeptides, termed aetheramides A (**1**) and B (**2**) (Figure 1). Their structures were elucidated by extensive NMR and ESIMS analysis, chemical derivatizations, and combined analysis of homonuclear (H−H) and heteronuclear (C−H)[2,3] *J*-couplings and quantum mechanical calculations.

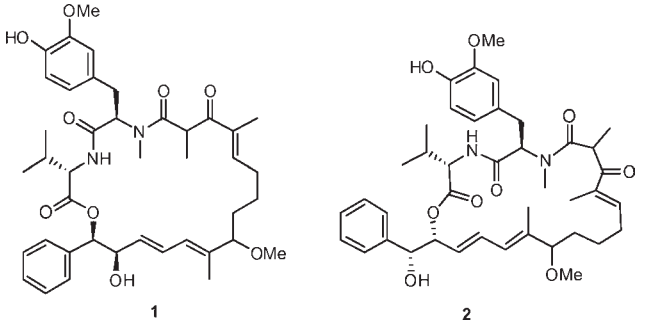

Figure 1. Structure of aetheramides A (**1**) and B (**2**).

HRESIMS of aetheramide B (**2**) displayed an $[M + H]^+$ peak at *m*/*z* 719.3920 (calcd for $C_{41}H_{55}N_2O_9$, 719.3908), consistent with the molecular formula $C_{41}H_{54}N_2O_9$. Its IR spectrum displayed absorption bands at 3367 and 1673 cm^{-1}, suggesting the presence of hydroxyl and carbonyl functionalities. The ^{1}H NMR spectrum of **2** in DMSO-d_6 (Table S1) exhibited signals characteristic of a peptide containing a polyketide section including an exchangeable NH proton at δ 8.13 (1H, d, J = 8.3 Hz), an *N*-methyl amide at δ 2.96 (3H, s), and two vinyl methyls at δ 1.65 (3H, s) and 1.55 (3H, s). Additionally, a downfield pair of triplets at δ 7.32 (2H, t, J = 7.5 Hz) and 7.23 (1H, t, J = 7.5 Hz) and a doublet at δ 7.39 (2H, d, J = 7.5 Hz), characteristic of a phenyl group, were observed. The HSQC spectrum revealed the presence of two α-amino methines ($\delta_{C\text{-}1}$ 58.8, $\delta_{H\text{-}1}$ 3.92, $\delta_{C\text{-}7}$ 54.9, $\delta_{H\text{-}7}$ 5.50), three oxygenated methines ($\delta_{C\text{-}26}$ 84.9, $\delta_{H\text{-}26}$ 3.48, $\delta_{C\text{-}33}$ 78.5, $\delta_{H\text{-}33}$ 5.38, $\delta_{C\text{-}34}$ 73.1, $\delta_{H\text{-}34}$ 4.77), and four olefinic methines ($\delta_{C\text{-}22}$ 140.4, $\delta_{H\text{-}22}$ 6.45, $\delta_{C\text{-}30}$ 126.7, $\delta_{H\text{-}30}$ 5.80, $\delta_{C\text{-}31}$ 130.2, $\delta_{H\text{-}31}$ 6.44, $\delta_{C\text{-}32}$ 127.5, $\delta_{H\text{-}32}$ 5.60). A detailed analysis of the 2D NMR spectra (HSQC, HMBC, COSY, and 2D-HOHAHA) confirmed the presence of a peptidic fragment (C1−C15) composed by valine and a rare 3-(4-hydroxy-3-methoxyphenyl)-2-(methylamino)propanoic acid (m*N*MeTyr) (see Figure 2). The remaining fragment (C16−C40) was identified as a polyketide containing three spin systems (A−C) shown in Figure 2.

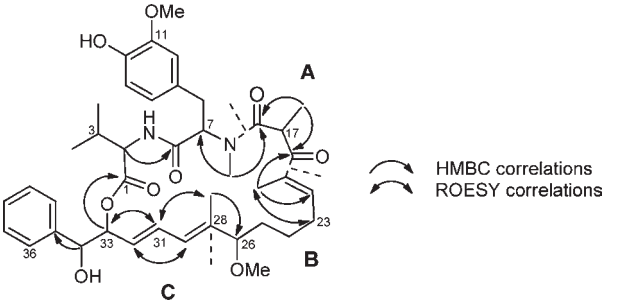

Figure 2. NMR-based connectivity of the fragments of aetheramide B (**2**). Fragments A−C are indicated by dashed lines. Key HMBC correlations used to connect the fragments and ROESY correlations used to determine the geometry of the double bonds are indicated by single- and double-sided arrows, respectively.

Key HMBC correlations from the upfield methyl doublet at δ 0.58 (3H, d, J = 6.7 Hz) and from the methine proton at δ 4.24 (1H, q, J = 6.7 Hz) to the carbonyl carbon at δ 171.7 (C-16) and ketone carbon at 197.2 δ (C-19) allowed us to determine the presence of a 2-methyl-3-oxopropanoic acid residue (A). On the basis of HSQC-TOCSY and COSY correlations, it was clear that spin system B started with an olefinic methine ($\delta_{H\text{-}22}$ 6.45, $\delta_{C\text{-}22}$ 140.4) and continued with three sequential methylenes and an oxymethine ($\delta_{H\text{-}26}$ 3.48, $\delta_{C\text{-}26}$ 84.9). Spin system C contained a conjugated diene ($\delta_{H\text{-}30}$ 5.80, $\delta_{C\text{-}30}$ 126.7, $\delta_{H\text{-}31}$ 6.44, $\delta_{C\text{-}31}$ 130.2, $\delta_{H\text{-}32}$ 5.60, $\delta_{C\text{-}26}$ 127.5) and two oxymethine groups ($\delta_{H\text{-}33}$ 5.38, $\delta_{C\text{-}33}$ 78.5, $\delta_{H\text{-}34}$ 4.77, $\delta_{C\text{-}34}$ 73.1). HMBC correlations from the proton at δ 4.77 to the aromatic carbon resonances at δ 141.3 (C-35) and 126.6 (C-36) extended this spin system to a phenyl ring. The complete structure of **2** was established from interpretation of a single HMBC experiment. Long-range correlations from the methyl group at δ 1.55 (H-29) to the sp^2 carbon signals for C-28 (δ 138.7) and C-30 and to the carbon resonance at δ 84.9 linked fragments C and B, while connectivity of fragment B to A was determined by HMBC correlations from the vinyl methyl at δ 1.65 (H-21) to the carbon resonances at δ 140.4 and 197.2. Thus, the polyketide fragment in **2** was identified as the unusual 14,15-dihydroxy-9-methoxy-2,4,10-trimethyl-3-oxo-15-phenyl-pentadeca-4,10,12-trienoic acid (Dmpp). Moreover, connectivity of the β-keto acid residue to the N-terminus of m*N*MeTyr was indicated from an HMBC correlation between the methyl amide proton at δ 2.96 and the

(4) Garcia, R; Gerth, K; Stadler, M; Dogma, I. J., Jr.; Müller, R *Mol. Phylogenet. Evol.* **2010**, *57*, 878.

(5) (a) Gerth, K; Steinmetz, H; Höfle, G; Jansen, R *Angew. Chem., Int. Ed.* **2008**, *47*, 600. (b) Wenzel, S. C.; Müller, R *Nat. Prod. Rep.* **2009**, *26*, 1385.

(6) Garcia, R. O.; Krug, D.; Müller, R. *Methods in Enzymology*; Hopwood, D., Ed.; Academic Press: Burlington, MA, 2009; Vol. 458, Chapter 3, pp 59−91.

carbonyl at δ 171.7. The downfield oxymethine proton at δ 5.38 (H-33) suggested a carboxylic acid ester at this position, and it was confirmed by an HMBC correlation from H-33 to the carbonyl carbon of valine (δ 169.4), thereby completing the structure of **2** as a 21-membered ring.

The absolute configurations of L-Val and D-m*N*MeTyr were assigned by chromatographic analysis (UV and TIC) of the L- and D-FDLA (1-fluoro-2,4-dinitrophenyl-5-leucinamide) derivatives of the acid hydrosylate of **2** (advanced Marfey's method).[7] Several techniques were used to determine the configuration of the stereocenters of the polyketide fragment. A $^{3}J_{H-H}$ coupling constant of 15.1 Hz between H-31 and H-32 indicated a *trans* disubstituted olefin. The *E* geometries of the $\Delta^{28,30}$ and $\Delta^{20,22}$ trisubstituted olefins were deduced from strong ROE correlations between Me-29 and H-31 and between Me-21 and H-23a, respectively. The relative configurations of the stereocenters at C-33 and C-34 were established by using a combination of *J*-based configurational analysis,[8] quantum mechanical calculations of the homo- and heteronuclear *J*-coupling values,[9a−c] and ROESY correlations. The heteronuclear coupling constants were accurately measured from *J*-resolved HMBC[10] and HETLOC[11] experiments, and ROE correlations were obtained from ROESY and HSQC-ROESY.[12] ^{1}H NMR data of **2** recorded in CD_3CN displayed a relatively large $^{3}J_{H-H}$ of 6.6 Hz between H-33 and H-34 indicating an anti relationship between these protons. Therefore the *threo* configuration between the hydroxyls at C-33 and C-34 was deduced from ROE correlations between H-32/H-36, H-33/H-36, and H-32/H-34 (Figure 3A).

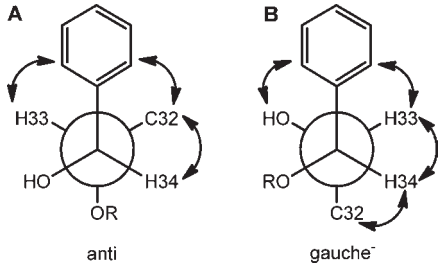

Figure 3. Newman projections, ROE correlations, and $^{3}J_{H-H}$ and $^{2,3}J_{C-H}$ values used to assign the *threo* configuration of C33/C34 in (A) **2** and (B) **1**.

According to Murata's method[8] aetheramide B shows $^{2}J_{C-H}$ values that may be classified as "medium" (−3.5 for H-34/C-33 and −3.4 Hz for H-33/C-34). Thus, we additionally determined the relative configuration at C-33/C-34 by using a combined NMR-quantum mechanical calculations approach. This method has proven to be useful in establishing the configuration of stereogenic centers within a macrocycle and in cases where the calculated[2,3]J_{C-H} cannot be qualitatively classified as "large" or "small".[13] The relevant *J* values for all possible configurations (three *syn* and three *anti* rotamers) of the C-33/C-34 stereocenters at the DFT MPW1PW91/6-31G(d,p) level (see Computational Details in the Supporting Information) were calculated and quantitatively compared to the experimental ones. Table 1 shows that the lowest total absolute deviation (TAD) value ($\Sigma|J_{calcd} - J_{expt}|$) corresponds to the *threo* anti arrangement. This result confirms the configuration determined by the *J*-based analysis presented above. The determination of the configurations of the remaining stereocenters (C-17 and C-26) could not be unambiguously defined by our spectroscopic analysis. A subsequent attempt, involving quantum mechanical calculations of the ^{13}C chemical shifts of the four possible stereoisomers and their comparison with the experimental counterpart,[9d,e] did not reveal sufficient evidence for a safe stereoassignment of C-17 and C-26, leaving therefore open their determination by total synthesis.

Table 1. Calculated and Experimental *J* Values (Hz) for the Fragment C-32/C-35 in **2**

	calculated[a]						
	erythro			threo			
	anti	g^{-c}	g^{+d}	anti	g^{-}	g^{+}	exptl[b]
$^{3}J_{H33-C35}$	3.1	1.0	5.1	1.4	5.2	1.1	2.6
$^{2}J_{H34-C33}$	−1.7	−2.9	4.0	−3.3	−3.0	3.1	−3.5
$^{3}J_{H33-H34}$	7.6	2.3	2.7	7.6	5.5	2.5	6.6
$^{2}J_{H33-C34}$	−2.3	1.2	−5.1	−4.0	−3.5	1.0	−3.4
TAD	4.4	11.1	15.6	**3.0**	4.3	16.6	

[a] MPW1PW91/6-31G(d,p) calculated *J* values. [b] Experimental values obtained from *J*-resolved HMBC, HETLOC, and HSQMBC spectra. [c] Gauche^{-}. [d] Gauche^{+}. Total absolute deviation (TAD) values calculated from the equation ($\Sigma|J_{calcd} - J_{expt}|$). Stereoisomer displaying lowest TAD value appears in bold.

Aetheramide A (**1**) eluted from the C12 HPLC column shortly before **2**. Its molecular formula was determined to be $C_{41}H_{54}N_2O_9$ by HR-ESI-MS (719.3912 $[M + H]^+$, calcd for $C_{41}H_{55}N_2O_9$, 719.3908) indicating **1** to be an isomer of **2**. Furthermore, 2D NMR data for **1** closely resembled those of aetheramide B with the exception of slight changes in the resonances belonging to the valine residue and the fragment C25−C35 (see Table S2). Indeed an HMBC correlation between the oxymethine proton at

(7) (a) Fujii, K.; Ikai, Y.; Oka, H.; Suzuki, M.; Harada, K.-I. *Anal. Chem.* **1997**, *69*, 5146. (b) Fujii, K.; Ikai, Y.; Mayumi, T.; Oka, H.; Suzuki, M.; Harada, K.-I. *Anal. Chem.* **1997**, *69*, 3346.
(8) Matsumori, N.; Kaneno, D.; Murata, M.; Nakamura, H.; Tachibana, K. *J. Org. Chem.* **1999**, *64*, 866.
(9) (a) Bifulco, G.; Bassarello, C.; Riccio, R.; Gomez-Paloma, L. *Org. Lett.* **2004**, *6*, 1025. (b) Bifulco, G.; Dambruoso, P.; Gomez-Paloma, L.; Riccio, R. *Chem. Rev.* **2007**, *107*, 3744. (c) Bagno, A.; Rastrelli, F.; Saielli, G. *J. Phys. Chem. A* **2003**, *107*, 9964. (d) Barone, G.; Duca, D.; Silvestri, A.; Gomez-Paloma, L.; Riccio, R.; Bifulco, G. *Chem.—Eur. J.* **2002**, *8*, 3240. (e) Di Micco, S.; Chini, M. G.; Riccio, R.; Bifulco, G. *J. Org. Chem.* **2010**, *8*, 1411.
(10) Meissner, A.; Soerensen, O. W. *Magn. Reson. Chem.* **2001**, *39*, 49.
(11) Uhrin, D.; Batta, G.; Hruby, V. J.; Barlow, P. N.; Koever, K. E. *J. Magn. Reson.* **1998**, *130*, 155.
(12) Bax, A.; Davis, D. G. *J. Magn. Reson.* **1985**, *63*, 207.
(13) (a) Plaza, A.; Bifulco, G.; Keffer, J. L.; Lloyd, J. R.; Baker, H. L.; Bewley, C. A. *J. Org. Chem.* **2009**, *74*, 504. (b) Plaza, A.; Bifulco, G.; Masullo, M.; Keffer, J. L.; Collin, P. L.; Hooper, J. N. A.; Bell, L. J.; Bewley, C. A. *J. Org. Chem.* **2010**, *75*, 4344.

δ 5.91 (H-34) and the valine carbonyl resonance at 169.4 (C-1) indicated an ester linkage at this position, therefore establishing the structure of **1** as a 22-membered lactone ring. $^3J_{H-H}$ coupling values and ROE data analysis confirmed the *E* geometries for all the olefins, while the absolute configurations of L-val and D-m*N*MeTyr were determined by the advanced Marfey method. *J*-based configuration analysis was used to establish the relative configuration at C-33/C-34. Indeed, a combination of a small $^3J_{H-H}$ of 0.8 Hz between H-33 and H-34 and small $^2J_{C-H}$ coupling constants of 0 Hz measured between H-34/C-33 and H-33/C-34 suggested a *threo* gauche$^-$ (g^-) configuration (Figure 3B). This result was fully supported by ROE correlations between H34/H32, H-33/H-36, OH-33/H-36, and H-33/H-34 (Figure 3B) and by the quantum mechanical calculations approach (see Table S4). Moreover, these results are in agreement with the configuration established for aetheramide B.

Similarly to the thuggacins, a family of macrolide lactones isolated from *Sorangium cellulosum*,[14] aetheramide A rearranges into aetheramide B (and vice versa) when dissolved in MeOH. This transesterification reaction occurs spontaneously, and within 24 h the equilibrium 1:1 is reached. It is also worthwhile to note that the presence of both aetheramides in freshly prepared extracts of fermentation broths and cell pellets was confirmed by LC-MS and NMR analysis.

To determine the absolute configuration at stereocenters C-33 and C-34, the modified Mosher method was applied to aetheramide B.[15] Treatment of **1** with an excess of *R*- or *S*-α-methoxy-α-trifluoromethylphenylacetic acid (MTPA) for 24 h yielded the respective bis-MTPA esters. Analysis of ^{1}H NMR chemical shift differences ($\Delta\delta_{S-R}$) from the ^{1}H NMR, COSY, and HSQC spectra (Figure 4 and Table S5) revealed that the absolute configuration at C-33 is *R* and therefore the absolute configuration at C-34 was also established as *R*.

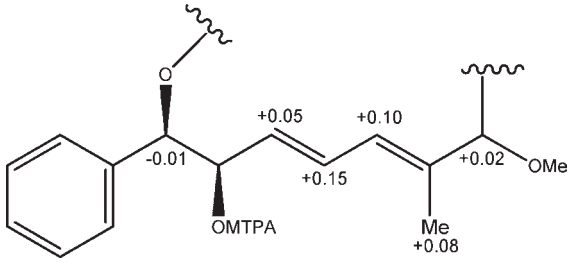

Figure 4. $\Delta\delta_{S-R}$ values (ppm) for the C-33 MTPA esters of **1**.

Aetheramides were screened for antibacterial, antifungal, cytotoxic, and anti-HIV activity. The effect of aetheramides on HIV-1 was evaluated by infecting the indicator cell-line TZM-bl with the HIV_{LAI} isolate according to established procedures (Figure 5).[16] Indeed, aetheramides A (**1**) and B (**2**) potently inhibited HIV-1 with an IC_{50} value of 0.015 and 0.018 μM, respectively. Measuring ATP levels as a parameter of cell viability of TZM-bl cells resulted in IC_{50} values of 0.14 μM for **1** and of 0.12 μM for **2**. Furthermore, **1** showed cytostatic activity toward the human colon tumor cell line HCT-116 with an IC_{50} value of 0.11 μM. The cytostatic activity of aetheramide B was practically identical to that observed for **1**. Aetheramides also exhibited moderate antifungal activity against *Candida albicans* at loads of 20 μg/disk.

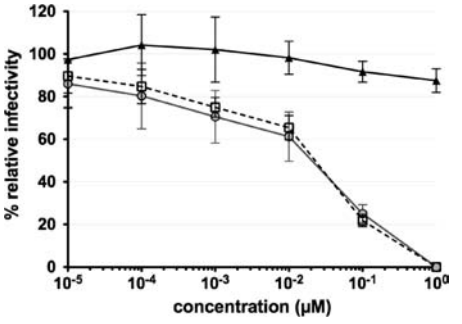

Figure 5. HIV-1 inhibition by aetheramides A (**1**) and B (**2**). The mean relative decrease in HIV infectivity in TZM-bl cells is given as a function of increasing drug concentrations. Gray circle, **1**; open box, **2**; black triangle, DMSO control. Error bars are standard deviations of four independent measurements.

In summary, aetheramides are a new class of antiviral natural products isolated from the new myxobacterium strain SBSr003 that belongs to the recently discovered genus "*Aetherobacter*". Aetheramides are cyclic depsipeptides that contain the unique structural polyketide moiety Dmpp and two amino acid residues including the unusual 3-(4-hydroxy-3-methoxyphenyl)-2-(methylamino) propanoic acid. Thus, the discovery of aetheramides from a new myxobacterial genus and their potent HIV-1 activity represent another example of the enormous biosynthetic capabilities of these microorganisms and their importance in drug discovery programs.

Acknowledgment. Work in the laboratory of R.M. was supported by the Bundesministerium für Bildung und Forschung (Grant No. 0315798) and the Deutsche Forschungsgemeinschaft. J.P.M. and A.M. were supported by the Spanish Ministry of Science and Innovation (SAF2010-21336).

Supporting Information Available. Experimental details, computational details, ^{1}H and ^{13}C NMR assignments, and 1D and 2D NMR spectra for **1** and **2**. This material is available free of charge via the Internet at http://pubs.acs.org. The authors declare no competing financial interest.

(14) Steinmetz, H.; Irschik, H.; Kunze, B.; Reichenbach, H.; Höfle, G.; Jansen, R. *Chem.—Eur. J.* **2007**, *13*, 5822.

(15) Hoye, T. R.; Jeffrey, C. S.; Shao, F. *Nat. Protoc.* **2007**, *2*, 2451.

(16) Brass, A. L.; Dykxhoorn, D. M.; Benita, Y.; Yan, N.; Engelman, A.; Xavier, R. J.; Lieberman, J. *Science* **2008**, *319*, 921.

The authors declare no competing financial interest.